ANL-5360
Metallurgy and Ceramics

-1-

ARGONNE NATIONAL LABORATORY
P. O. Box 299
Lemont, Illinois

SOME THEORETICAL FACTORS IN THE ZONE MELTING PROCESS

by

Richard J. Dunworth

METALLURGY DIVISION

Published

February, 1956

Operated by The University of Chicago
under
Contract W-31-109-eng-38

DISCLAIMER

2

SOME THEORETICAL FACTORS IN THE ZONE MELTING PROCESS

by

Richard J. Dunworth

INTRODUCTION

Zone melting is a process recently developed by Pfann[4] for the purification of metals. The method removes solute elements to such a degree that a metal may be obtained of purity higher than hitherto possible. Trace elements may be concentrated to an amount sufficient for analytical detection. The process may also be used to homogenize alloys. Certain phase-diagram information, such as eutectic composition and peritectic formation at low solute concentrations, can be determined. Zone melting is an important research tool and, in the transistor industry, of indispensable commercial value.

Purification of an alloy by zone melting depends on the difference in solute concentration between the liquid phase and the solid phase. A long rod of the alloy is laid horizontally in a boat. A small length of the rod is melted and this molten zone is made to move along the rod as shown in Fig. 1. If purification is desired, the zone is moved repeatedly in the same direction; the greater the number of passes, the greater the purification. Increased purification is obtained as the ratio L/z increases, where L is the length of the rod and z the length of the molten zone. Solutes that lower the melting point of the system ($k < 1$) concentrate in the last zone, while solutes that raise the melting point ($k > 1$) concentrate in the first zone. The distribution coefficient, k, shown in Figure 2, is defined by

$$k = \frac{C_s}{C_L} \quad , \tag{1}$$

where C_s is the solute concentration in the solid and C_L is the solute concentration in the liquid. As k approaches 1, the purification obtained in a given system becomes less.

Other factors that influence the purification are: the diffusion rates of the solute in the solid and liquid phases; the degree of thermal or magnetic stirring in the liquid zone; the irregularity of the solidifying interface; a concentration gradient in the liquid near the interface. These factors relate to solidification phenomena and will be discussed in the second section. The first section will treat of the mechanics of the theoretical separation obtained by varying k, L/z, and the number of passes.

3

SECTION I. THEORY OF ZONE MELTING

The mathematical treatment of zone melting was first described by Pfann.[4] Subsequent papers by the same author [5, 6, 7, 8, 9] described experiments and additions to the theory for transistor manufacture. Additional solutions of the zone melting equations are presented by Lord, [11] Reiss,[12] and Burris.[37] The latter paper presents excellent graphs for a certain number of passes and relatively small L/z ratios, such as may be encountered in laboratory practice.

The type of segregation obtained by normal freezing has been discussed by Scheuer,[1] Hayes and Chipman,[2] McFee,[3] and Pfann.[4] This segregation is described by the equation [derived in the Appendix (page 29)],

$$C_s = k\, C_0 (1 - g)^{k-1} \quad , \qquad (2)$$

where C_0 is the initial concentration in the rod, g is the fraction solidified, and C_s and k have the same meaning as before. A schematic drawing of a metal rod solidifying by normal freezing is shown in Figure 3. Initially, the rod was melted completely and freezing has progressed to a certain fraction, g, as shown in the drawing. The process continues until all the metal has frozen progressively from the one end. Curves showing solute distribution as a result of normal freezing are shown in Fig. 4. Improved purification, as k becomes much greater than 1 or much less than 1, is quite evident. Equation 2 depends on the following assumptions: (1) Diffusion in solid negligible; (2) Diffusion in liquid complete; (3) k is constant, i.e., does not vary over the composition range of interest; (4) Equilibrium distribution of solute between the solid just freezing and the liquid is obtained. Purification by normal freezing can be accomplished by cropping 20% or 30% of the solute rich end and repeating the purification of the purer end. This method is a batch operation and wasteful of the solvent metal. The great advantage of zone melting is that it is continuous and conserves the maximum amount of the solvent metal.

Zone Refining Process

The zone melting process differs from the normal freezing process in that only a small length or zone of the bar is molten at any one time. Greater purification is obtained by normal freezing than by a single pass of the molten zone through a bar. This may be shown by comparing the curves in Fig. 4 for normal freezing with the curves in Fig. 5 for a single pass of the zone. The difference is due to the fact that the small zone becomes enriched more rapidly in solute than the longer molten bar. After five passes (Fig. 6), however, the zone melting process has resulted in considerably more purification than that obtained by one normal freezing cycle. After 10 passes, or at the ultimate purification (Fig. 9), there is no longer any value in comparing the two processes. It may be noted that the theoretical curves are all derived on the basis of the assumptions listed for Equation 2.

4

In addition to these assumptions the following are also required for zone melting: (1) a constant zone length and (2) a constant cross-sectional area.

An equation may be derived for the first pass of a zone melted bar (Appendix, p. 31):

$$C_{s(1)} = C_0 + \gamma e^{-\alpha x} \tag{3}$$

where $\alpha = k/z$, $\gamma = D_{(1)}\alpha - C_0$, $D_{(1)} = z C_0$, x = distance zone has travelled from the front of the rod, and the subscript (1) refers to the first pass. Equation 3 describes the concentration, C_s, at any point, x, in the frozen solid (shown in Fig. 1). This equation represents an integration of the zone melting process up to the point, x. A small increment of solid charge, dz, of composition C is melted and added to the liquid zone, z, of uniform composition, C_L. At the same time a small amount of solid, dx, of composition, kC_L, freezes and is added to the frozen solid. These solid increments (dx) increase in concentration until the concentration C_L equals C_0/k ($k C_L = C_0$). Then the concentration frozen in dx equals the concentration melted in dz and no further change in C_L is obtained. A uniform concentration is maintained along the remainder of the bar until the last zone is reached. This is illustrated by the curves in Fig. 5 for k = 0.5, 0.6, 0.7, and 0.8. In the last zone all the solid charge has been melted and the solute distribution is given by Equation 2 for normal freezing.

Equations have been developed for the 2nd, 3rd, and succeeding passes. The derivation is similar to equation 3 and is given in the Appendix, pp. 31, 32:

$$C_{s(2)} = C_0 + (\alpha\gamma x e^{-k} + \delta)\, e^{-\alpha x} \tag{4}$$

where $\delta = D_{(2)}\alpha - C_0$, $D(2) = z\int_0^z C_{s(1)}\, dx$

and

$$C_{s(3)} = C_0 + \left(\alpha^2 e^{-2k}\gamma \frac{(x+z)^2}{2} + \alpha e^{-k}\delta x + \epsilon\right) e^{-\alpha x} \tag{5}$$

where $\epsilon = D_{(3)}\alpha - C_0 - \frac{k^2}{2}\gamma e^{-2k}$, $D_{(3)} = z\int_0^z C_{s(2)}\, dx$.

The equations for the succeeding passes become quite complicated and laborious to solve. Since the terms $\gamma, \delta, \epsilon, \ldots$ are negative, the number of significant figures required is quite large for values of C_s below 10^{-4}. These objections also apply to the equations developed by Lord.[11] Furthermore, neither set of equations is applicable in the last zone and apply only to that section of the bar not affected by the normal freezing in the last zone. This section, L', of the bar is given by the relation

$$L' = L - nz \tag{6}$$

where n is the number of passes. After 10 passes, then, the last 10 zones are not computed by the equations. A method of pass by pass computation may be used as a good approximation. The solute concentration frozen out at any point, x, is given by kC_L. In Figure 1, dx and dz are usually chosen equal to one half the zone length or one zone length. The amount of solute added to the liquid zone by melting dz is found from the C_s curve of the preceding pass. The amount of solute frozen out is estimated and then checked by a material balance at the point calculated. This method of calculation was used to obtain the data for Figures 6 and 8 which show the distribution after 5 passes for $k < 1$ and $k > 1$, respectively. In all the graphs z was equal to 0.1 L, which was the value used in the experimental runs.

After a large number of passes, a distribution is reached that additional passes will not change. This curve is called the ultimate distribution and, if $k < 1$, is given by the equation

$$C_s = Ae^{Bx} \text{ where } A = C_0 \frac{BL}{e^{BL}-1} \tag{7}$$

$$e^{Bz} = \frac{Bz}{k} + 1 \quad .$$

If $k > 1$, the distribution is given by

$$C_s = Ae^{-Bx} \text{ where } A = C_0\, BL \tag{8}$$

$$k = \frac{Bz}{1-e^{-Bz}} \quad .$$

Equations 7 and 8 are derived in the Appendix, p. 33. It may be noted that semi-logarithmic plots of equations 7 and 8 result in straight lines. These equations are plotted in Figs. 9 and 10 for various values of k. Although the lines are plotted through the last zone (from x = 9 to x = 10), the values are not accurate. More exact values for the last zone may be obtained by using Equation 2 and calculating the distribution for normal freezing. The value of C_0 in Equation 2, used in this calculation, is the difference between the amount originally present in bar (10 gm/cc) and the amount frozen out in the solid up to the point x = 9. This amount is given by an integration of Equation 7 from x = 0 to x = 9 or by noting that, at the point x = 9, the amount of solute in the zone must equal $C_s(x = 9)/k$. The difference is greater between the values given by Equation 7 and Equation 2 as k approaches zero or infinity. In Fig. 11 the values obtained from these equations are plotted for k = 0.5 and, in Fig. 12, for k = 0.1. The practical significance of the shape of the curve in the last zone is slight, however, when it is considered that both curves represent the same amount of solute and the last zone undoubtedly will be discarded.

6

The more rigorous solution to the zone melting equation described by Burris[37] takes the shape of the last zone into account in calculating the ultimate distribution curve. In Tables 1, 2, and 3, values listed by Burris are compared with values obtained from the solution of Equations 7 and 8. In Figs. 11 and 12 a comparison is made between values obtained from Equation 2 and values from Burris' paper. The agreement in the values calculated by different methods is quite good, especially in a practical range of the distribution coefficient ($5 > k > 0.1$). Again, when discussing solute concentrations, it seems of little practicality to dispute about values (listed in Table 3 for $k = 10$ and $x = 9$) differing by a factor of 10^2 when the absolute value is 10^{-38}. It is an extremely small amount of solute in either case. The factor of 2 difference (in Table 1 for $k = 0.1$ and $x = 0$) has as little significance. In Table 2, where the L/z ratio is only 5, the effect of the last zone is more important and a greater difference is shown in the values listed. In most experimental or commercial applications of zone melting, in which the distribution coefficient, k, will lie between 0.1 and 5, and the L/z ratio will be greater than 10, the rapid calculation by Equations 7 and 8 will more than compensate for the slight inaccuracies inherent in their use.

The existence of an ultimate distribution curve, first postulated by Pfann,[4] and later shown by Burris[37] in pass by pass calculations, may be deduced with the aid of Fig. 13. In this diagram, $k = 0.1$, $L = 10$, $z = 1$ and $C_0 = 1$. At the point $x = 1.8$, we have a concentration of solute in the solid of $C_{s(1)} = 6.6\ (10^{-12})$ and a liquid zone, z_1, of solute concentration $C_{L(1)} = 6.6\ (10^{-11})$ as, by definition, $C_s = kC_L$. After the zone, z_1, has moved a short distance Δx we may enter the zone melting equation with values taken from the graph and solve for $C_{L(2)}$.

$$C_{L(2)} = C_{L(1)} + \Delta z\ \overline{C_{s(3)}} - \Delta x\ \overline{C_{s(4)}} \qquad (9)$$

or

$$C_{L(2)} = C_{L(1)} + \Delta x \left[C_{s(3)} - C_{s(4)}\right]$$

$$\text{as} \quad \Delta x = \Delta z \quad .$$

This equation merely states that the amount of solute in the zone after solidifying a volume Δx and melting a volume Δz equals the amount initially present plus the amount dissolved in Δz minus the amount frozen in Δx. Solving Equation 9 we obtain $C_{L(2)} = 9.6\ (10^{-11})$ and consequently $C_{s(2)} = 9.6\ (10^{-12})$. This is the value of $C_{s(2)}$ obtained from Equation 7. A similar calculation at any point on the curve will produce the same results. There is, therefore, no change in the curve and the ultimate distribution has been reached. As shown by Burris,[37] the earlier passes follow the ultimate distribution curve from the last zone to the front as shown by the dashed curve in Fig. 13. A calculation on this curve for $C_{s(1)}$ and $C_{s(2)}$ results in $C'_{s(1)}$ and $C'_{s(2)}$ of lower value showing that the ultimate

distribution has not been reached. Further passes will bring the values of $C'_{s(1)}$ and $C'_{s(2)}$ into agreement with $C_{s(1)}$ and $C_{s(2)}$ of the ultimate distribution curve. Only one set of points will satisfy Equation 7, since it was derived on this basis.

The number of passes to obtain the ultimate distribution depends on the purification ratio, L/z, and the distribution coefficient. The number of passes required increases as the ratio L/z increases and as k approaches 1. By using the value of C_s at x = 0 on the ultimate purification curve, the necessary passes may be estimated. If, in each pass, each value of C_s (at x = 0) were equal to k C_s of the preceding pass, the total purification would be equal to k^n (where n is the number of passes). Because of the length of the zone, only a certain percentage of this theoretical limit is attained. In Table 4, percentages are listed for several k's. It is evident that, as k approaches one, the efficiency drops off quite rapidly. For example, in Fig. 9, C_s is 10^{-14} at x = 0 for the curve k = 0.1 If $k^n = 10^{-14}$, fourteen passes would be required. An efficiency factor of 75% (taken from Table 4) increases the number of passes required to 18.6 (= 14/0.75). Similarly for k = 0.5, C_s is 10^{-5}; $k^n = 10^{-5}$; and n = 16.6; and correcting n for percent efficiency, we have 16.6/0.50 = 33.2 passes required. As k approaches one, the ultimate purification is less for a greater number of passes.

The preceding treatment describes the theory of zone melting using the optimum conditions obtainable. The many assumptions, on which the equations are based, are not entirely justified. Negligible diffusion of solute in the solid state and constant k are two assumptions that, in many cases, are not going to be sources of great error. Considerable difficulty is encountered, however, in maintaining a constant zone length and equal cross sectional area throughout the rod --- at least in laboratory melting. It may be expected that, in certain commercial applications, these conditions may be met and this source of error removed. The assumptions of complete diffusion in the liquid and equilibrium distribution of solute between liquid and solid phases are of considerable theoretical interest and will be discussed in next section.

SECTION II. SOLIDIFICATION STRUCTURE OF METALS

The structure of metal castings has been the subject of many investigations. The elimination of macro defects such as shrinkage, pipe, porosity and segregation has been a primary concern. The size, orientation and shape of the cast grain structure are discussed in some papers. Recently, attention has been directed to developing theories of solidification by examining atomic movement at the liquid-solid interface. Zapfee[27] postulates the presence of micelles or atomic blocks in the liquid. As freezing progresses, these micelles are attached to the interface much in the same manner as bricks are laid to build a wall. The subcrystalline imperfections or mosaics and the cleavage facets observed on fractured surfaces are the evidence on which Zapfee bases this theory. The size of the micelles is of the order of 10^{-5} cm, which would make cubes of 300 atoms to a side. The more popular theory assumes that a continuous and rapid interchange of atoms takes place between the solid and liquid phases as described by Turnbull[21] and Chalmers.[25, 29, 30] The latter theory provides the basis for the following discussion.

Rate of Freezing

Freezing progresses and the interface advances as heat is removed through the solid metal. The probability that an atom will become attached to the interface is defined as the accommodation coefficient by Chalmers.[25] The body-centered cubic structures have higher accommodation coefficients than the close-packed structures - face-centered cubic and hexagonal close-packed. Where the type of crystal bonding is partially covalent (e.g., silicon and germanium), the accommodation coefficient is quite low. The calculated rate of advance of the interface, for a slight amount of supercooling, is very fast. Evidence for the rapid growth rates may be deduced from Turnbull's work[42] on supercooled alloy droplets. The small Cu-Ni drops were supercooled about 300° C before solidification started. Dendritic growth was observed near the surface of the small drops where freezing was most rapid. It is difficult to conceive of dendritic formation at very rapid growth rates without postulating a greater velocity to the atom that is solidifying than to the freezing interface. The rate of advance of the solidifying interface is dependent more on the rate of extraction of the latent heat of fusion than on the time required for atom movement from the liquid phase to the solid phase.

If a face-centered cubic crystal is considered, the accommodation coefficient of the (111), (100), and (110) planes would be in the ratio 1:1.5:2 (Chalmers[25]). Then the following relations are postulated:

$$R_{F\ (111)} < R_{F\ (100)} < R_{F\ (110)} \tag{10}$$

$$T_{F\ (111)} < T_{F\ (100)} < T_{F\ (110)} \tag{11}$$

where R_F is the rate of freezing, T_F is the equilibrium temperature for freezing, and the subscript refers to the plane on which the freezing process is occurring. Depending on the initial orientation, either a (111) or a (100) plane will predominate in the interface at the expense of the faster growing planes which grow out of existence. [See also Turnbull,[21] Desch.[38]] If the accommodation coefficient is approximately equal to the area in the plane not occupied by atoms, the values for face-centered cubic planes would be: (111) - 0.093; (100) - 0.215; (110) - 0.44. For the same body-centered cubic planes, the values are: (111) - 0.28; (100) - 0.41; (110) - 0.17. It would be expected that the axis of the columnar grains found in cast metals would be in the [111] direction for face-centered metals or in the [110] direction for body-centered metals. According to Barrett,[39] however, the columnar axis for both cubic systems is in the [100] direction. The same orientation is found in dendritic growth and a mechanism, similar to that described in the section on dendrites, may be postulated. For the rate of freezing, R_F, and the rate of melting, R_M, Chalmers[25] has developed the following equations:

$$R_F = A_F G_F \nu e^{-Q_F/RT} \tag{12}$$

$$R_M = A_M G_M \nu e^{-Q_M/RT} , \tag{13}$$

where A is the accommodation coefficient, G is the probability of atom vibration being in the right direction, ν is the vibration, Q is the activation energy, R is the gas constant and T is the absolute temperature. Using these equations Chalmers estimates that the R_F and R_M for copper at the melting point are about 3000 cm/sec; that is to say, the atoms leave or become attached to the solid at this speed. Of course, at the melting point R_F is equal to R_M. For one degree of supercooling, R_F is greater than R_M, and $R_F - R_M = 2$ cm/sec. By using other equations presented by Chalmers[25] it is possible to show that the following relation is approximately valid:

$$\frac{R_F}{R_M} = e^{(T_e - T)L/RTT_e} , \tag{14}$$

where T_e is the equilibrium temperature for the melting and freezing process and L is the latent heat of fusion. Equation 14 is derived in the Appendix, p. 34. Turnbull[21] derived an equation for the rate growth, G, of the solidifying interface and obtained the following equation:

$$G = \frac{\lambda kT}{h}\left(1 - e^{-\Delta F/RT}\right) , \tag{15}$$

where λ is the interatomic spacing, k is the Boltzman's constant, h is Planck's constant, and ΔF is the difference in free energy between atoms in the liquid and solid phases. The calculation of G for one degree of supercooling by Eq. 15 results in a value of 720 cm/sec (Appendix, p. 34). This rate differs by a factor of 360 from the value of 2 cm/sec but the rapidity of growth for one degree of supercooling is evident.

Supercooling

Supercooling in the liquid may be of two forms - thermal supercooling in which the temperature of the liquid is actually lower than the temperature at the interface; and constitutional supercooling resulting from a high concentration of solute at the interface. Constitutional supercooling was mentioned by Chipman[2] and later developed mathematically by Chalmers[13] and Wagner.[24] The effects of constitutional supercooling are considered by Chalmers in many papers.[14, 15, 17, 28, 31]

Figure 14 shows schematically freezing conditions in which no supercooling exists. The thermal gradient near the interface is relatively flat according to Chalmers,[25] who measured the gradient with a thermocouple in the bar. The temperature of the liquid does rise, however, and is higher than the interface temperature at all points. It may be assumed that most of the superheat in the liquid and the latent heat of fusion are extracted through the solidified metal in a direction to the left (in Fig. 14). The conditions for thermal supercooling are shown in Fig. 15. The direction of freezing is the same as in Fig. 14. The temperature in the liquid is lower than the interface temperature (T_I) at every point. In order to accomplish this type of supercooling an appreciable amount of heat must be extracted from the liquid by radiation or conduction. It is probable that a large amount of the heat will continue to be removed through the solidified metal. It is not likely, in the zone melting process, that any thermal supercooling can occur. Since the heat is generated in the molten zone, it is fairly certain that the temperature of the liquid will be greater than the interface temperature. If the molten zone becomes very large in comparison to the length affected by the heater, and if the rate of solidification becomes very rapid, some thermal supercooling might occur in the liquid near the interface. The zone length should be the same length or smaller than the heater length to eliminate any possibility of thermal supercooling.

Constitutional supercooling is a relatively new concept in solidification of alloy systems. Although postulated some time ago by Chipman[2] it was not until recently that much experimental data was offered to support the theory. Constitutional supercooling is used to explain much of the phenomena observed in alloy solidification by Chalmers,[13, 14, 15, 16, 17, 25, 28, 29, 30, 31] Hall,[40] Burton,[41] and Ruddle.[43] Constitutional supercooling is caused by an increased concentration of solute atoms at the interface due to non-equilibrium freezing conditions. This increase results from the fact that

11

the diffusion rate of the solute atoms into the liquid zone is less than the rate of freezing. Calculations by Chalmers[13] showed that as little as 0.01% of solute is sufficient to cause a slight amount of constitutional supercooling but that a slow freezing rate or a steep temperature gradient will eliminate a small alloy effect. The presence of hexagonal projections on the solid-liquid interface, observed by Pond and Kessler,[18] Chalmers[14, 15] and Prince,[35] lends support to the possibility of supercooling at very low alloy concentrations. In alloys of appreciable solute concentration the presence of dendrites in the cast structure can be explained by a solute concentration gradient at the interface.

According to Jost,[23] diffusion coefficients in the liquid state are 10^{-5} cm^2/sec within a factor of 10. The following systems are listed: Mg in Al at 700°C; Au in Bi at 500°C; Au, Rh, and Pt in Pb at 500°C; Ag, Au and Pb in Sn at 500°C. The diffusion coefficient of Si in Fe, however, is 2.4 (10^{-5}) cm^2/sec at 1480°C and 10.8 (10^{-5}) cm^2/sec at 1560°C. While not very many systems have been studied, the consistency is good if compared with the diffusion coefficients in the solid state. Substitutional diffusion coefficients vary from 10^{-8} to 10^{-12} cm^2/sec and interstitial diffusion coefficients vary from 10^{-6} to 10^{-8} cm^2/sec. A freezing rate of 0.04 cm/hr (1/64"/hr) would balance a diffusion rate of 10^{-5} cm/sec. Most of the work described by Chalmers has been done at freezing rates of 6 cm/hr to 60 cm/hr, or about 100 to 1000 times the average diffusion rate.

To obtain constitutional supercooling, the concentration gradient of solute, in the vicinity of the interface, will be as shown in Fig. 16. A molten zone is pictured with the different solute concentrations designated by C. At the left of the figure, the concentration curve of the solute in the solid, frozen after the passage of the molten zone through distance, x, is given by C_S. At the interface between liquid and solid just freezing, the concentration of solute in the solid is $C_{S(I)} = k\, C_{L(I)}$. C_L' is the concentration in the liquid at any distance x' from the interface. C_L is the concentration in the bulk of the liquid and C_0 is the concentration of the feed rod at the right in Fig. 16. The point $C_{S(I)}$ is very nearly equal to C_0. In a short distance, $C_{S(I)}$ will equal C_0, equilibrium will be obtained between the freezing solid and the melting solid, and $C_{S(I)}$ will be a constant value as in zone melting theory. The difference is, of course, that C_L is much less than C_0/k and the total purification is less. The effect is to make the experimental distribution coefficient, k_{exp}, closer to one. The dashed line, at the left is the curve which would be followed by the solute distribution in the solid if the theoretical distribution coefficient were followed.

Equations have been developed by Chalmers[13] and Wagner[24] to describe the concentration gradient shown in Fig. 16. According to Chalmers,

$$C_L' = C_{L(I)}\, e^{-Rx'/D} + C_L \quad , \tag{16}$$

12

where R is the rate of freezing and D is the diffusion coefficient. In Fig. 16, the characteristic distance, L_C, is defined as the distance, x', at which

$$C_{L'} = \frac{1}{e} C_{L(I)} + C_L \qquad (17)$$

so that

$$L_C = D/R \quad . \qquad (18)$$

If D is approximately 10^{-5} cm^2/sec, then L_C varies from 0.0003" to 0.003" as R varies from 10"/hr to 1"/hr. The distance over which this concentration gradient operates is probably of the order of fluid film thicknesses. If this is the case, an increase in agitation would have little effect on the concentration peak. The experiments of Burton,[41] however, show that agitation results in an improvement in purification, presumably by lowering the solute concentration at the interface. The maximum value of the solute concentration at the interface is obtained when equilibrium has been established between the concentration of the solidifying metal and the concentration of the melting metal, i.e., $C_{S(I)}$ equals C_0. This value of the interface concentration is given by the equation

$$C_{L(I)} + C_L = C_0/k \quad . \qquad (19)$$

A greater amount of solute will thus result in more supercooling. As an example, choose k = 0.1; if C_0 = 0.1% then $C_{L(I)} + C_L$ = 1%; if C_0 = 1%, $C_{L(I)} + C_L$ = 10%. There is, however, little change in L_C with increased solute and the shape of the exponential curve is essentially the same in both cases.

The method by which the concentration gradient produces supercooling may be seen in Fig. 17. In the top half of the diagram, the concentration gradient in a liquid zone is shown as well as the gradient in part of the freezing solid on the left and the melting solid on the right. The bottom half of the diagram is a plot of the temperature gradient in the rod (heavy line) superimposed on the solidus and liquidus temperatures (dashed line). The amount of supercooling is represented by the cross-hatched area. It must be remembered that the diagram is out of proportion and that L_C is about 10^{-2} or 10^{-3} of the zone length, z. The effect of constitutional supercooling on the shape of interface and the segregation of solute depends on the depression of the temperature at the interface, ΔT, coupled with the fact of slight temperature gradient in the liquid. The difficulty in the equation is that the freezing rate produces a greater effect than predicted by the equation. The term, R, in the equation should probably be squared.

13

Hexagonal Cellular Structures

The formation of projections on the freezing interface has been observed by Chalmers[14] and Pond[18] in castings solidified slowly from one end. The longitudinal striae or corrugations on the surface of the casting are other sections of the same structure. It is believed that constitutional supercooling causes these projections. This structure is formed in a certain range of freezing rates, slight thermal gradient and a sufficient amount of solute impurity.

The projections extend 1 mm into the liquid when a tin alloy of either 0.1% Pb or 0.1% Sb is frozen at a rate of 0.7 cm/min [Chalmers[14]]. The projection is then 100 times the distance, L_C, described by Equation (18).

The amount of solute present has a definite effect on the spacing of the surface striations and thus on the diameter of the projection. Goss[36] found that in Sn of 99.997% purity the spacing was about 0.004" at a rate of growth of 1.2"/hr. If 0.01% to 0.1% of Ag, Cd, Zn, or Pb were added to the liquid tin, the spacing was much broader. An addition of 1% Sb or In, which are more soluble in tin than these metals, produced very broad lines.

The size of the projection is also affected by the rate of growth of the interface. Growth rates in the range of 1"/hr to 30"/hr produced these hexagonal projections with about 0.1% solute impurity [Chalmers,[14] Pond,[18] and Goss[36]]. The more rapid growth produced smaller projections. If slower speeds than 1"/hr or faster speeds than 30"/hr were used, the projections disappeared. Prince,[35] however, observed similar projections in weld deposits of 18-10 Cr-Ni steel. At an estimated solidification rate of 200"/hr, the alloy content was sufficient so that the projections formed. These hexagonal projections can be explained satisfactorily by means of constitutional supercooling since the formation of the projection depends, to a marked degree, on the amount of solute present.

Dendrites

When a large amount of thermal or constitutional supercooling is present in the liquid, dendrites will grow into the liquid. Most alloy castings exhibit dendrite formation, as shown by Rhines,[19] Bever,[26] and Turnbull.[42] In certain alloys the primary dendrite phase will be broken up by subsequent phase changes. Dendrites are not found ordinarily in cast billets of pure metals but, under special conditions, Chalmers[16] was able to obtain dendrites in high purity lead castings.

The influence of various solidification factors on dendrite spacing was investigated by Rhines.[19] About 100 alloys of Al, Cu, Mg, and Sb in a composition range of 1% to 90% were examined for dendritic formation. The alloys were chill cast into cast iron molds and all the billets contained

14

certain dendritic types. The dendritic spacing increased with larger solute concentrations and slower growth rates. There was some tendency for the spacing to increase when the crystal structure of the solvent metal was more complex (less densely packed). There was no relation between dendritic spacing and grain size or freezing range. Rhines explains the formation of dendrites as growing from a single idiomorph at fast rates of growth. A corner of the idiomorph grows preferentially and develops into another crystal of the same size and shape as the original crystal. The growth continues in the direction of supercooling until a dendrite is formed. At slow rates of growth, the idiomorph increases in size uniformly with no preferential growth at the corner.

Chalmers[16] produced a dendritic structure in high purity lead by melting the lead in a horizontal boat and rapidly withdrawing the boat from the furnace. Apparently the liquid was supercooled sufficiently by radiation for the formation of dendrites. The model of dendritic growth proposed by Chalmers is a pyramid which is constructed of faces of closely packed planes. The pyramid extends rapidly into the liquid and the area of the base grows much more slowly. A bar is formed by this mechanism of square cross section and a pyramidal tip. The 111 planes that form the faces of the pyramid are the only ones that survive in the initial rapid growth. Loosely packed planes, that grow rapidly, grow out of existence. When the bar has grown to sufficient length, the formation of secondary and tertiary branches will depend on suitable conditions of supercooling being present in the vicinity of growth. Depending on the crystal structure there is a certain direction of dendritic growth. As listed by Chalmers,[16] for face-centered cubic and body-centered cubic lattices, dendrites grow in the [100] direction; hexagonal close-packed dendrites grow in the $[10\bar{1}0]$ direction; body-centered tetragonal (tin) in the [110] direction. Each direction forms the axis of a pyramid of closely packed planes.

The effect of dendritic growth on the purification obtained from zone melting could be quite serious. A considerable amount of liquid of high solute concentration might be entrapped between the dendrites. If short zone lengths are used, however, the amount of thermal supercooling, that will be produced, is negligible. According to Chalmers,[16] even very rapid, uniform rates of moving the boat did not produce dendrites, and it was necessary to remove the furnace completely before the structure was obtained. In induction heating, the maximum concentration of flux (and consequently temperature) is obtained at the center of the coil, and the temperature gradient in the liquid will necessarily be unfavorable to dendritic growth. If long zones (greater than 1") are considered desirable, a coil length should be chosen nearly equal to the length of the zone. Then the flux will be distributed over the zone length and a thermal gradient will be obtained that increases to the center of the zone.

It is more difficult, however, to reduce a high concentration of solute at the interface in order to eliminate constitutional supercooling. Here, again, the use of a coil equal in length to the zone length will tend to increase the stirring action at the freezing interface. The use of lower frequency induction equipment would also increase the mixing of solute. Mechanical or supersonic stirring might be beneficial. If the amount of solute is less than 0.1%, the constitutional supercooling will not be sufficient to form dendrites, but the hexagonal projections will be produced instead. These projections will tend to increase the area of the solidifying interface but not to entrap any liquid. It may be suspected that, in the zone melting process, a high concentration of solute at the freezing interface will reduce purification per se rather than through effects such as dendrites and hexagonal projections on the freezing interface.

Lineage structures or mosaics are defects found in single crystals grown from the melt. These markings are formed by arrays of dislocations in a direction parallel to the direction of heat flow. At higher rates of solidification the lineage boundaries tend toward the characteristic direction of dendritic growth. According to Chalmers,(15) the lineage boundary in tin tended to grow in the [110] direction. The actual direction of growth is a compromise between the direction of dendrite growth and the direction of heat flow. The effect of the lineage boundaries appear as striations on the surface and disappear at rapid growth speeds. The orientation may vary from 5 min to 2° between mosaic blocks. A mechanism for the formation of mosaics is shown in Fig. 18 [due to Chalmers(15)]. The direction of growth of two crystal faces is shown by the arrow. This direction is determined by the rate at which the planes AB and BC advance. In Fig. 18 (a), equal rates are postulated for both faces. The dashed lines indicate the position after a certain growth, g. Since the rate of heat transfer through the face BC is less than that through the face AB (as measured by the ratio of the projections of the faces, CD/AD), the position shown in Fig. 18 (b) is more likely. In this diagram the face BC has grown one half the amount of the face AB. If there were a great difference in accommodation coefficients between the two planes AB and BC, the resultant growth might be as shown in Figs. 18 (c) or 18 (d). In a consideration of mosaic structures where the orientation difference is slight, such a difference in the accommodation coefficients is hardly possible. If the two faces were of different crystals (as in polycrystalline material), however, the direction may be as described in Figs. 18 (c) or 18 (d). The line BB' would now be a grain boundary separating the crystals. The formation of columnar growth in castings proceeds by this method. This type of defect does not have any apparent effect on the purification obtained by zone melting.

16

Effective Distribution Coefficient

The effect of various solidification factors on the distribution coefficient has been investigated by Hall,[40] Burton(41) and McFee.[3] If k is less than one, the distribution coefficient approaches 1 as the rate of freezing increases and the purification obtained is less than that theoretically possible. The effective distribution coefficient may be plotted versus the rate of freezing and a curve will be obtained similar to that shown in Fig. 19. Two mechanisms may be proposed to explain this decrease. A concentration gradient of solute may exist in the liquid with the highest concentration at the interface. Solidification proceeds with k equal to the theoretical distribution coefficient, but the solid freezes from a liquid of high solute concentration. The effective k becomes greater than the theoretical k, and the purification is correspondingly lower. According to the other theory, solute atoms, in excess of the theoretical amount, become adsorbed or trapped on the interface. The interface is being bombarded by so many solvent atoms in the process of solidifying, that there is no opportunity for excess solute atoms to be released from the interface. It is probable that both mechanisms occur; the former process is dominant at slow speeds and the latter process is dominant at fast speeds.

The effective distribution coefficients of group III and group V elements in Ge and Si were measured by Hall.[40] In Ge the values were: B - 10; Al, P, Ga, As - 0.1; In, Sb - 0.002. In Si the values were: B - 0.9; Ga, As - 0.08; P - 0.05; Sb - 0.01; Al - 0.002; In - 0.0007. The coefficients of the group V elements (P, As, Sb) had more dependence on the speed of solidification than the group III elements. Hall also found a variation in k with the plane of growth, i.e., for the 111 plane, k = 0.010; for the 100 plane, k = 0.009; for the 110 plane, k = 0.008. The planes, 111:100:110, are in the same order as in Equation 10, where the 110 plane had the most rapid freezing rate, the highest equilibrium temperature for freezing and the highest accommodation coefficient. The first two factors contribute little to the distribution coefficient obtained, since the freezing rate was held constant and the diffusion rate probably was unchanged by the slight increase in freezing temperature. It is more likely that the distribution coefficients of the less densely packed planes, by virtue of higher accommodation coefficients, approach the equilibrium distribution coefficient more closely than the densely packed planes. Alternatively, it may be surmised that the different planes have different coefficients. Whichever supposition is correct, it has been demonstrated that there is a variation of distribution coefficient with the accommodation coefficient. In the zone melting of polygrain material, it may be expected that the distribution coefficient closest to one will be obtained as the 111 plane is presumed to be most numerous in the grains of the interface.

McFee[3] measured the rejection of K ion by growing crystals of NaCl at various freezing rates. The data are plotted in Fig. 19 as an example of distribution coefficient versus freezing rate experiments. It may

17

be expected that the freezing rate will be faster than shown in Fig. 19 when zone melting metallic alloys. The halogen compounds have very low accommodation coefficients due to the strong ionic bond in the crystal.

The experiments of Burton[41] on Sb in Ge provide evidence for the existence of a high concentration of solute near the interface. Burton was able to produce stirring at the interface by rotating the crystal as it was withdrawn from the melt. In this method of crystal growth, a certain amount of rotation is desirable so that a uniform cross section may be obtained. At a rotation of 57 RPM, the distribution coefficient changed from 3.5 (10^{-3}) to 8.6 (10^{-3}) as the freezing rate increased from 1-1/2"/hr to 10-1/2"/hr. At a rotation of 1440 RPM, however, the coefficient increased only slightly - from 3.1 (10^{-3}) to 3.8 (10^{-3}) with the same change in growth rate. It is interesting to note that even at a slow speed of 1-1/2"/hr some concentration gradient exists, as evidenced by the improved coefficient at 1440 RPM. These experiments and the formation of dendrites in cast alloy billets coupled with the absence of dendrites in cast pure metal billets, constitute the most important proofs for the existence of a concentration gradient at the solidifying interface.

Summary

In the first section, equations are presented for calculating solute distribution after zone melting. These equations are based on certain assumptions that may not be fully realized in practice. The difficulties in pass-by-pass calculation are given but the ultimate distribution may be obtained rather easily. A method is given for estimating the number of passes required to obtain the ultimate distribution.

In the second section, the influence of various solidification factors on the purification resulting from zone melting is described. The effect of hexagonal projections, if present, is considered to be slight and dendrites are presumed to be absent. The existence of a high solute concentration at the solidifying interface is demonstrated. The importance of this solute gradient on the purification is emphasized. The necessity of using slow rates of solidification or agitation to reduce the effectiveness of this gradient is shown.

COMPARISON OF VALUES FROM BURRIS' REPORT
WITH VALUES CALCULATED BY EQUATION 7

Table 1

$L = 10, z = 1, k < 1$

k	X = 0		X = 2		X = 5		X = 9	
	Burris	Equation 7	Burris	Equation 7	Burris	Equation 7	Burris	Equation 7
0.01	$2.02(10^{-27})$	$4.66(10^{-27})$	$8.03(10^{-22})$	$19.8\ (10^{-22})$	$1.55(10^{-13})$	$5.5\ (10^{-13})$	0.10	0.07
0.1	$4.25(10^{-15})$	$6.9\ (10^{-15})$	$5.71(10^{-12})$	$9.6\ (10^{-12})$	$2.80(10^{-7})$	$4.99(10^{-7})$	0.99	0.97
0.2	$5.30(10^{-11})$	$7.45(10^{-11})$	$1.07(10^{-8})$	$1.52(10^{-8})$	$3.04(10^{-5})$	$4.46(10^{-5})$	1.93	1.86
0.5	$4.43(10^{-5})$	$4.65(10^{-5})$	$5.35(10^{-4})$	$5.66(10^{-4})$	$2.19(10^{-2})$	$2.4\ (10^{-2})$	3.77	3.58

Table 2

$L = 10, z = 2, k < 1$

k	X = 0		X = 2		X = 5		X = 9	
	Burris	Equation 7	Burris	Equation 7	Burris	Equation 7	Burris	Equation 7
0.01	$6.77(10^{-14})$	$29.5\ (10^{-14})$	$3.37(10^{-11})$	$17.9\ (10^{-11})$	$9.14(10^{-7})$	$29.8\ (10^{-7})$	0.10	1.27
0.1	$1.28(10^{-7})$	$2.5\ (10^{-7})$	$4.59(10^{-6})$	$9.33(10^{-6})$	$1.14(10^{-3})$	$2.13(10^{-3})$	0.92	2.96
0.2	$1.43(10^{-5})$	$2.22(10^{-5})$	$2.03(10^{-4})$	$3.17(10^{-4})$	$1.14(10^{-2})$	$1.71(10^{-2})$	1.67	3.44
0.5	$1.05(10^{-2})$	$1.16(10^{-2})$	$3.67(10^{-2})$	$4.1\ (10^{-2})$	$2.43(10^{-1})$	$2.71(10^{-1})$	2.65	3.36

COMPARISON OF VALUES FROM BURRIS' REPORT WITH VALUES CALCULATED BY EQUATION 8

Table 3

$L = 10,\ z = 1,\ k > 1$

k	X = 0		X = 0.2		X = 0.5		X = 1		X = 5		X = 9	
	Burris	Equation 8	Burris	Equation 8	Burris	Equation 8	Burris	Equation 8	Burris	Equation 8	Burris	Equation 8
2	15.96	15.9	11.6	11.54	7.17	7.16	3.22	3.24	$5.37(10^{-3})$	$5.6(10^{-3})$	$8.47(10^{-6})$	$9.7(10^{-6})$
5	49.7	49.65	18.0	18.4	3.93	4.15	0.311	0.346	$4.74(10^{-10})$	$8.4(10^{-10})$	$1.13(10^{-21})$	$1.92(10^{-18})$
10	100	100	13.0	13.5	7.78	0.674	$3.66(10^{-3})$	$4.5(10^{-3})$	$3.96(10^{-23})$	$1.9(10^{-20})$	$1.15(10^{-38})$	$8.2(10^{-40})$

Table 4

% Efficiency of Multiple Passes

k	0.01	0.05	0.1	0.2	0.3	0.4	0.5	0.6	0.7	0.8	0.9
%	90	83	75	65	58	53	50	48	47	44	35

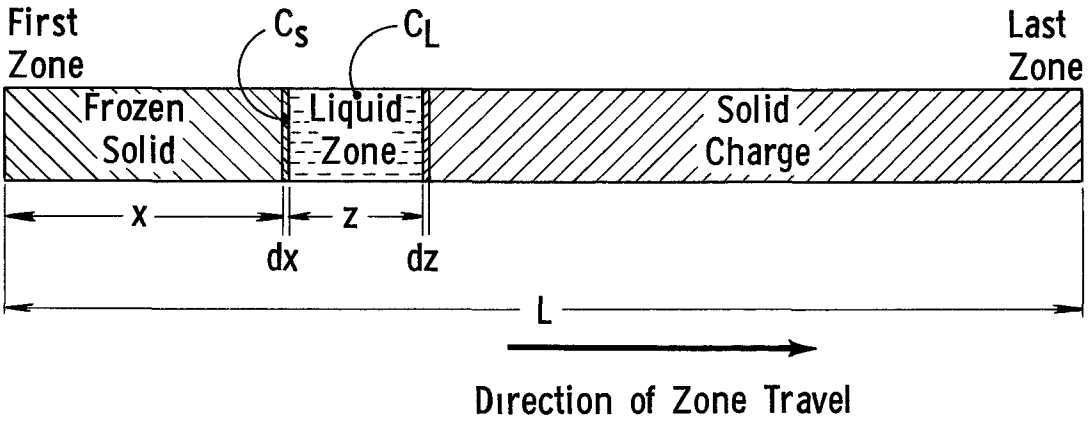

Figure 1

Molten Zone in a Metal Rod

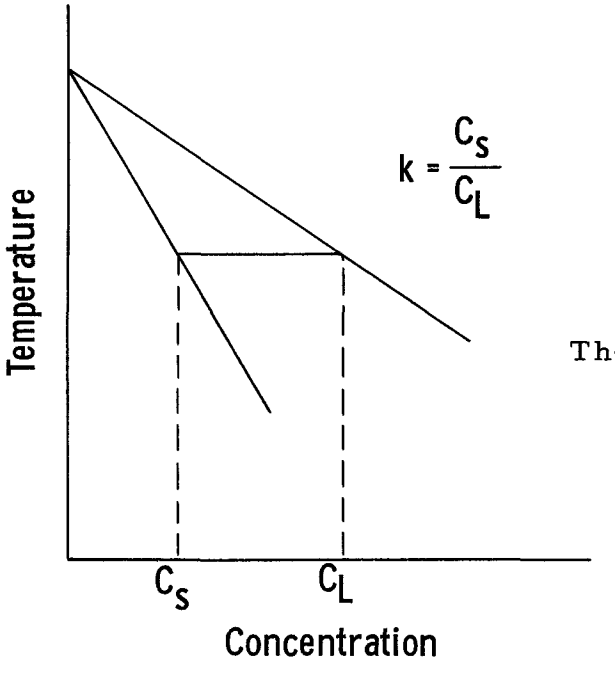

Figure 2

Theoretical Distribution Coefficient

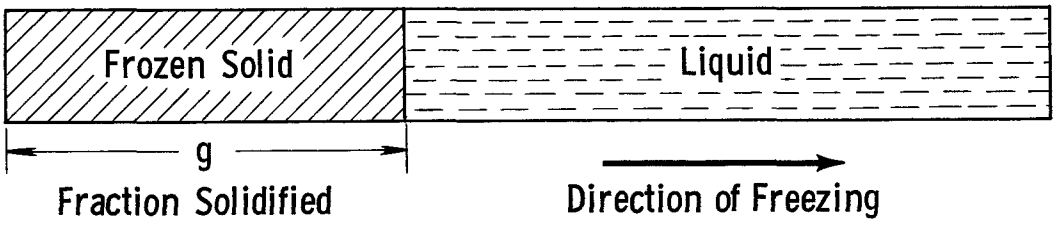

Figure 3

Normal Freezing of a Metal Rod

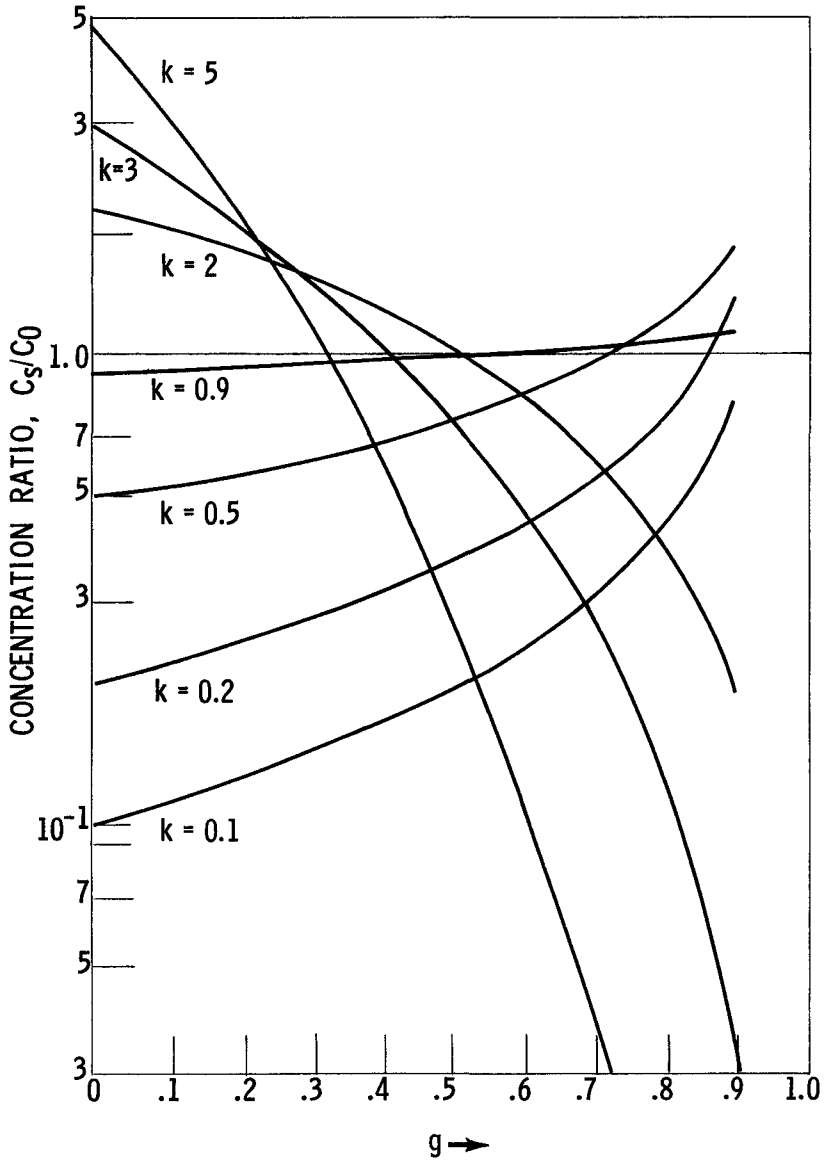

Figure 4

Concentration After Normal Freezing

L = 10, C_0 = 1

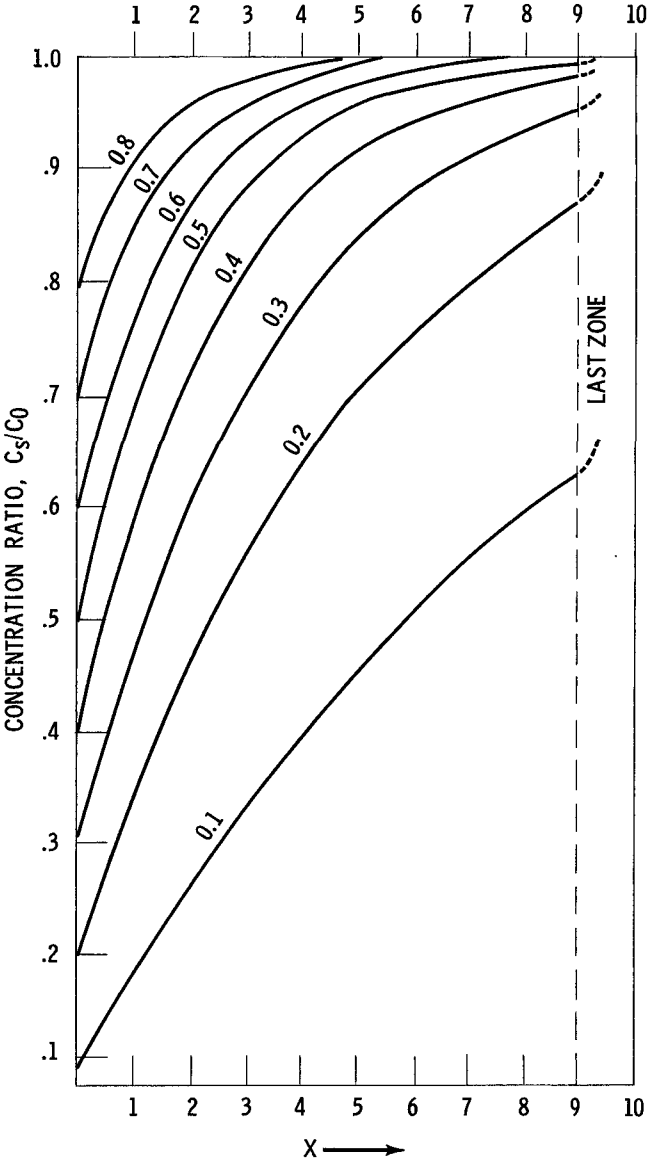

Figure 5

Concentration After 1 Pass of Zone Through the Rod

L = 10, C_0 = 1, z = 1, k = .1, .2, .3, .4, .5, .6, .7, .8

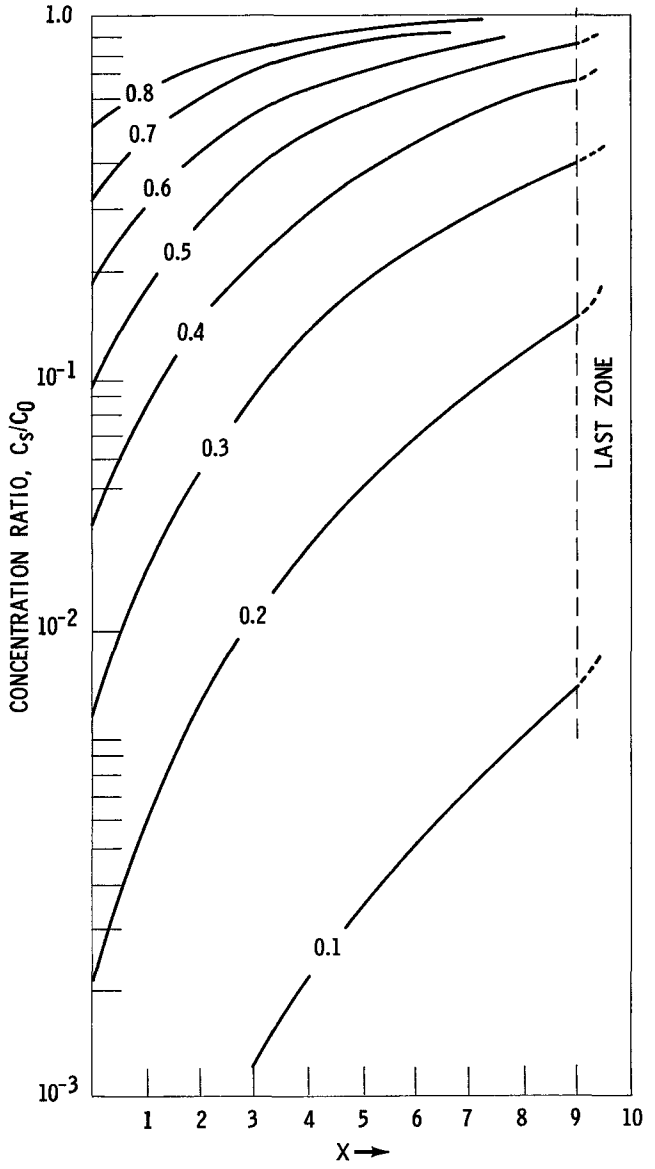

Figure 6

Concentration After 5 Passes of Zone Through the Rod

L = 10, C_0 = 1, z = 1,

k = 0.1, 0.2, 0.3, 0.4, 0.5, 0.6, 0.7, 0.8

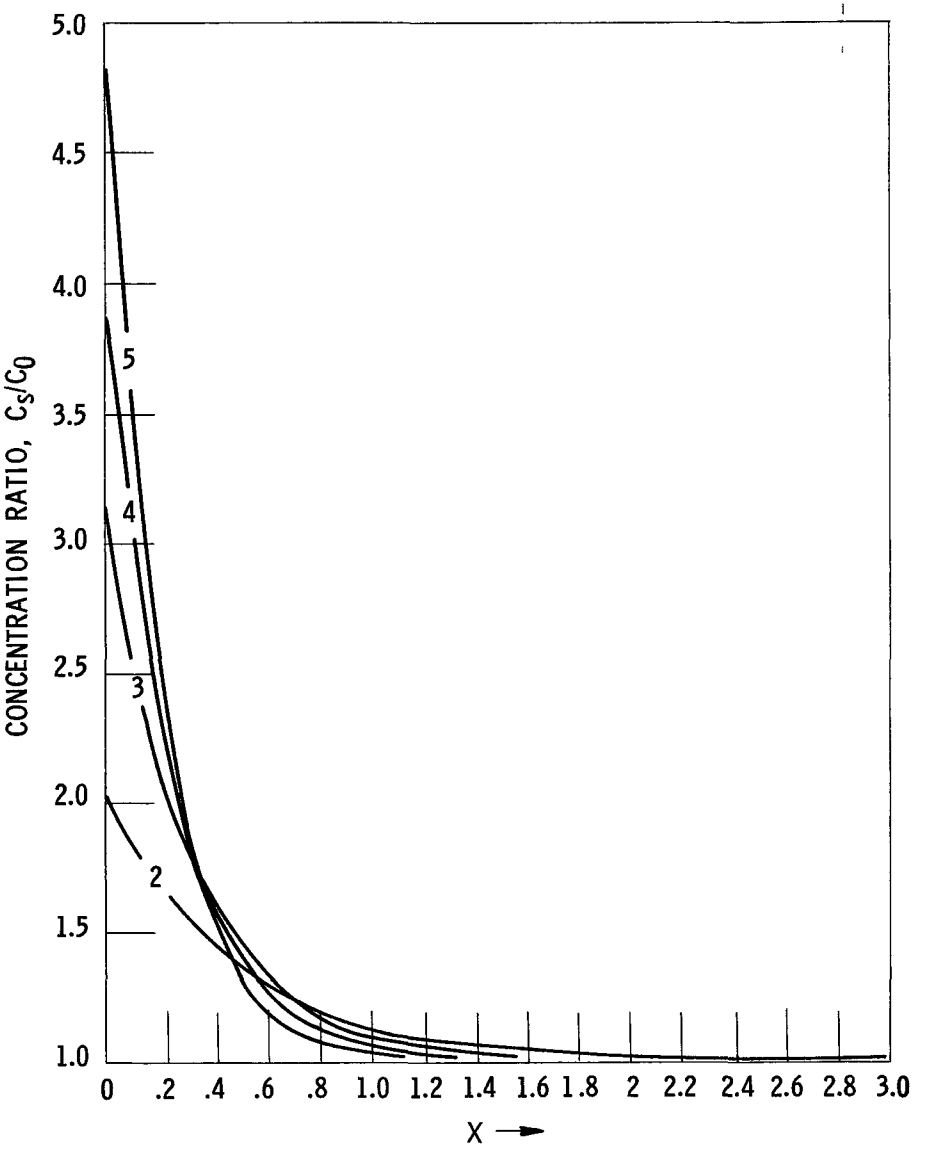

Figure 7

Concentration in First Three Zones After 1 Pass of the Zone Through the Rod

L = 10, C_0 = 1, z = 1, k = 2, 3, 4, 5

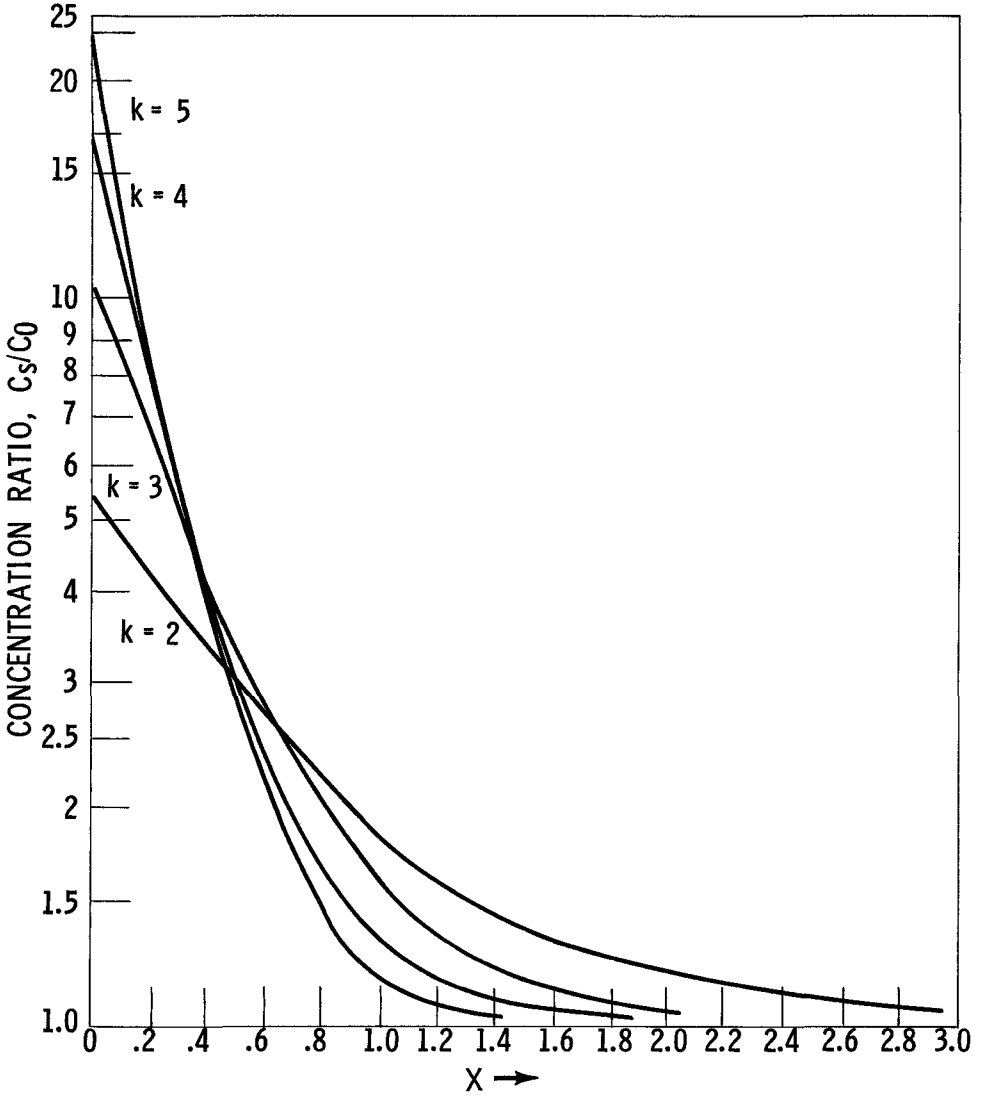

Figure 8

Concentration in First Three Zones After 5 Passes of the Zone Through the Rod

L = 10, C_0 = 1, z = 1, k = 2, 3, 4, 5

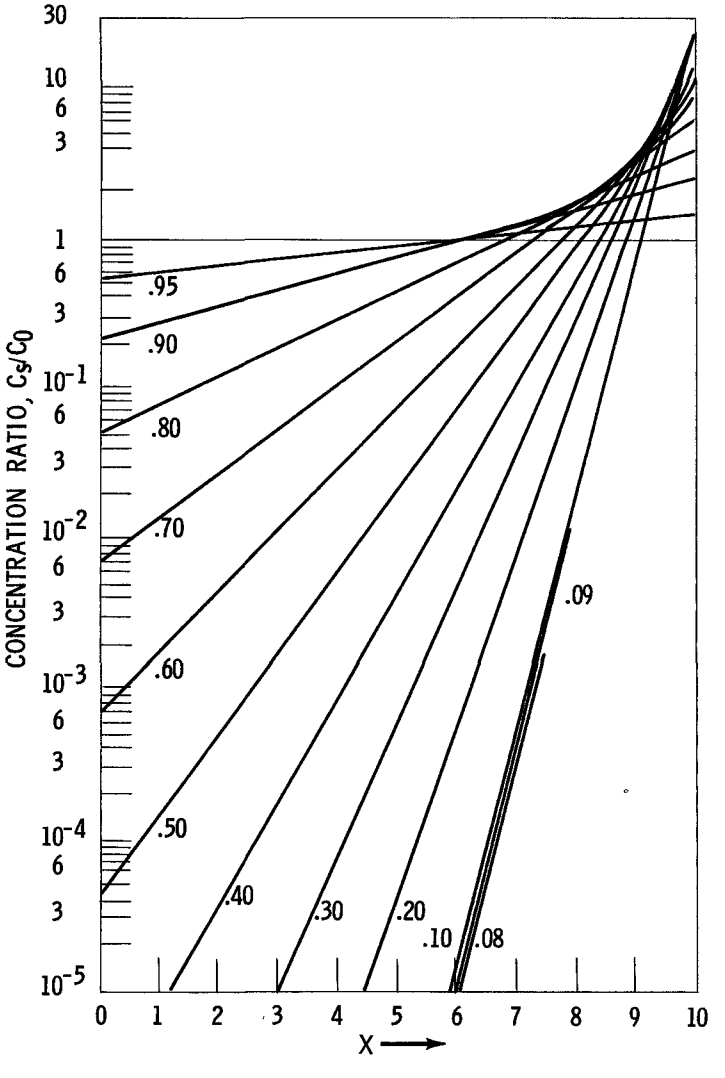

Figure 9

Ultimate Concentration Curves for Values of k Between 0.08 and 0.95

L = 10, C_0 = 1, z = 1

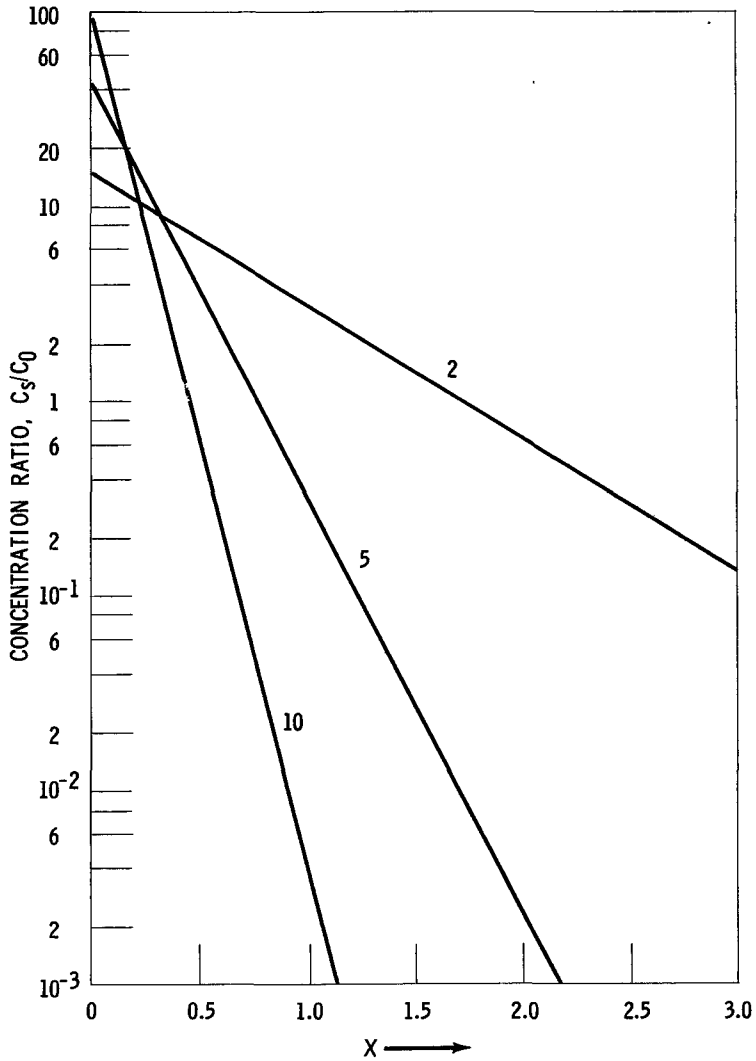

Figure 10

Ultimate Concentration Curves in the First Three Zones

k = 2, 5, 10

L = 10, z = 1, C_0 = 1

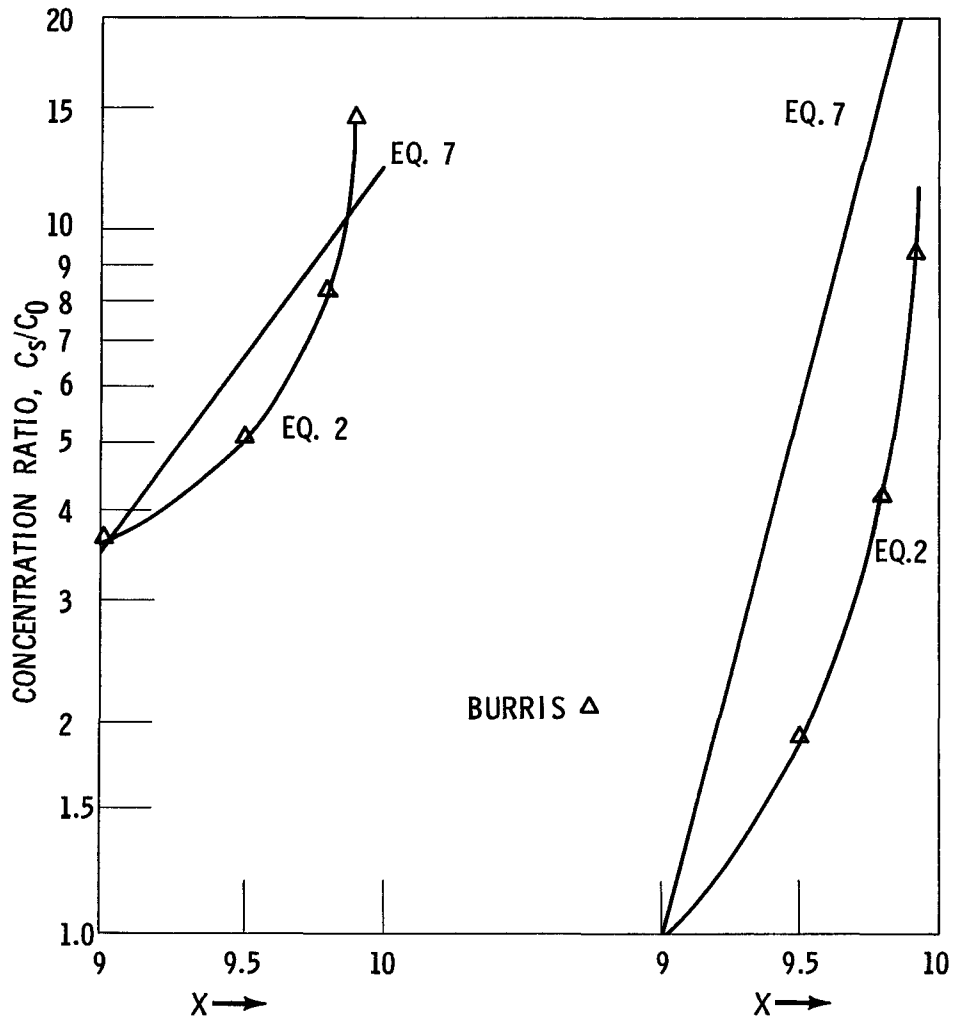

Figure 11
k = 0.5

Figure 12
k = 0.1

The Ultimate Concentration Curve in the Last Zone as Calculated by Equations 2, 7, and Burris

L = 10, C_0 = 1, z = 1

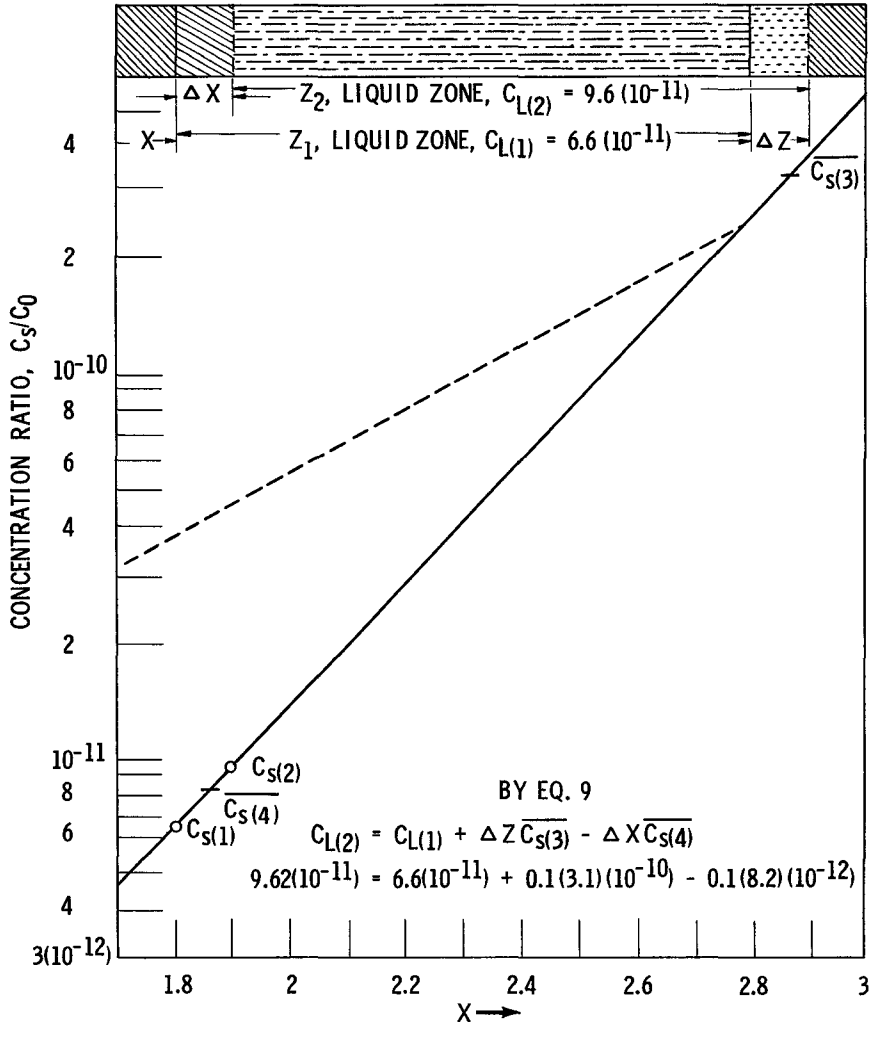

Figure 13

Analysis of Ultimate Concentration Curve

$k = 0.1$, $L = 10$, $z = 1$, $C_0 = 1$

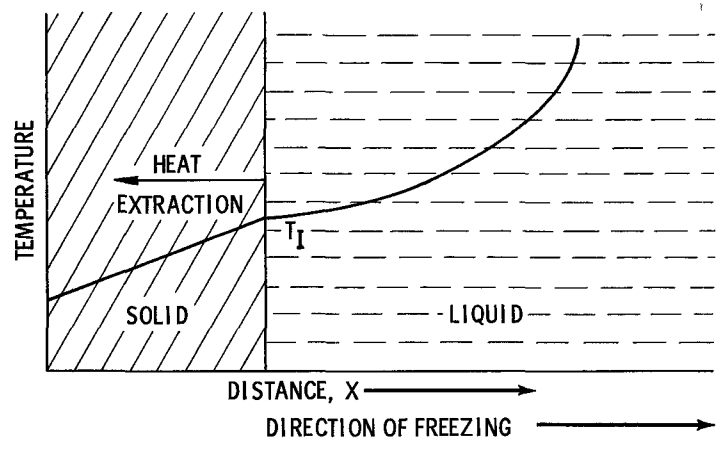

Figure 14

No Supercooling in Liquid

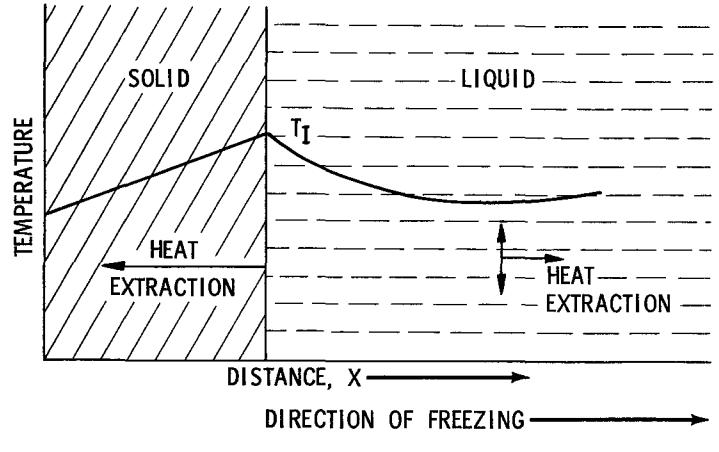

Figure 15

Thermal Supercooling in Liquid

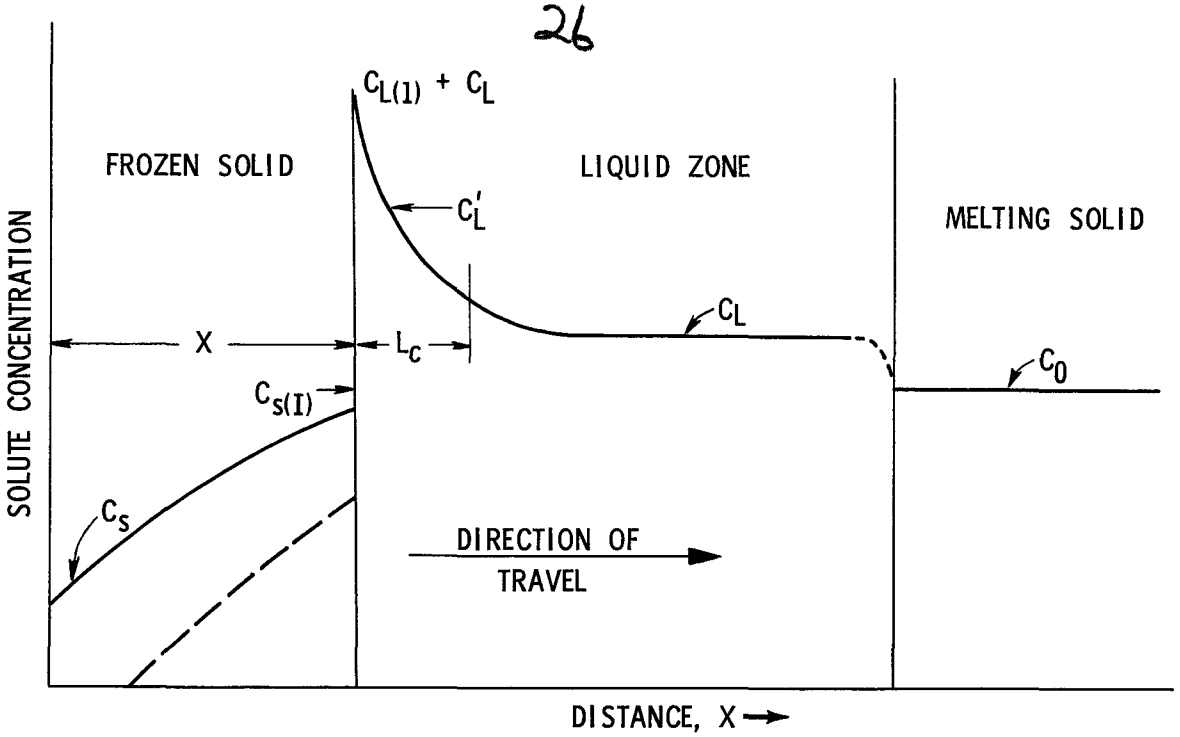

Figure 16

Increased Solute Concentration at the Solid-Liquid Interface During the Freezing Process

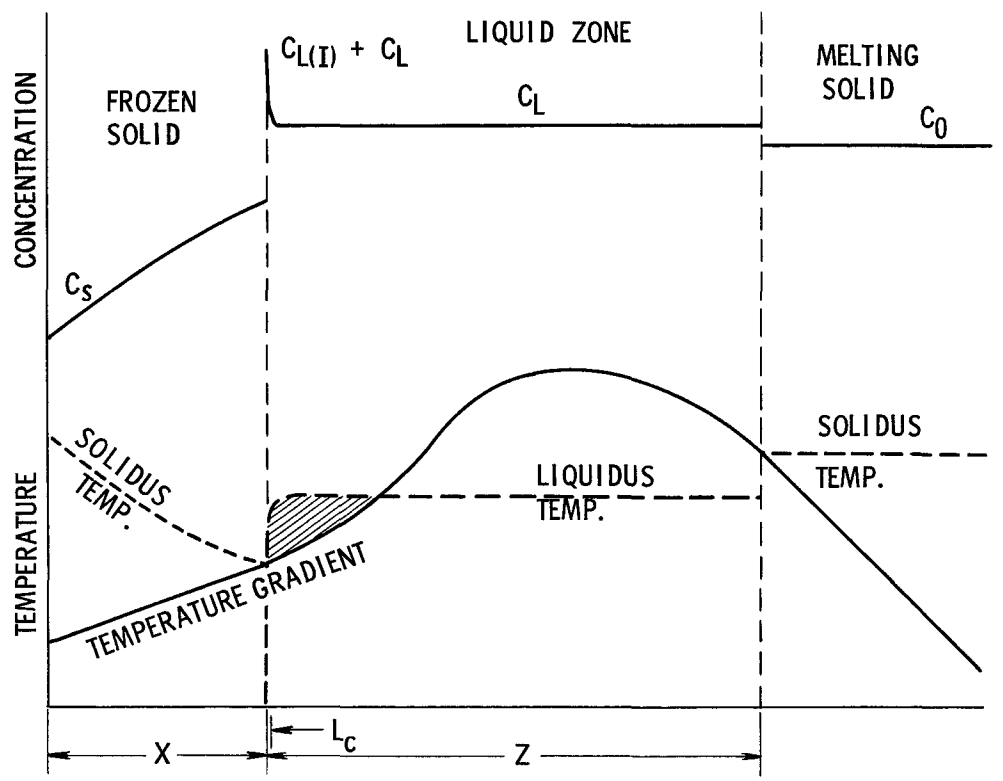

Figure 17

Constitutional Supercooling in Liquid, Shown by Crosshatched Area

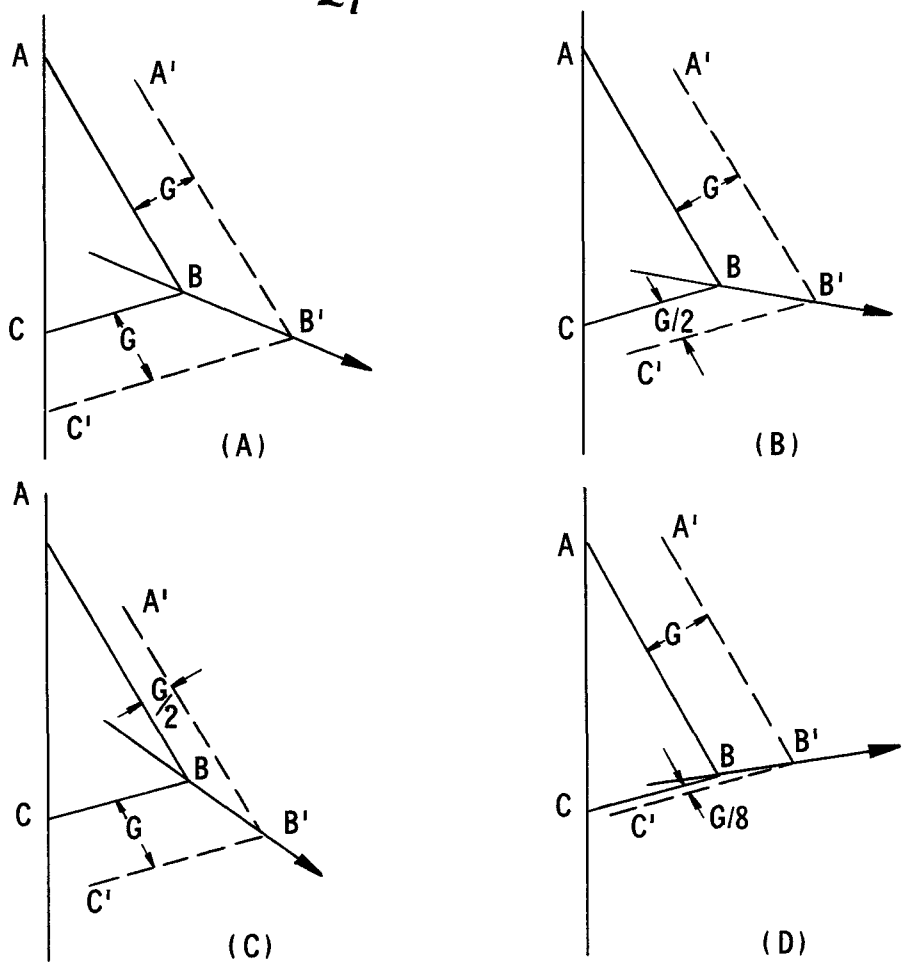

Figure 18

Direction of Crystal Growth

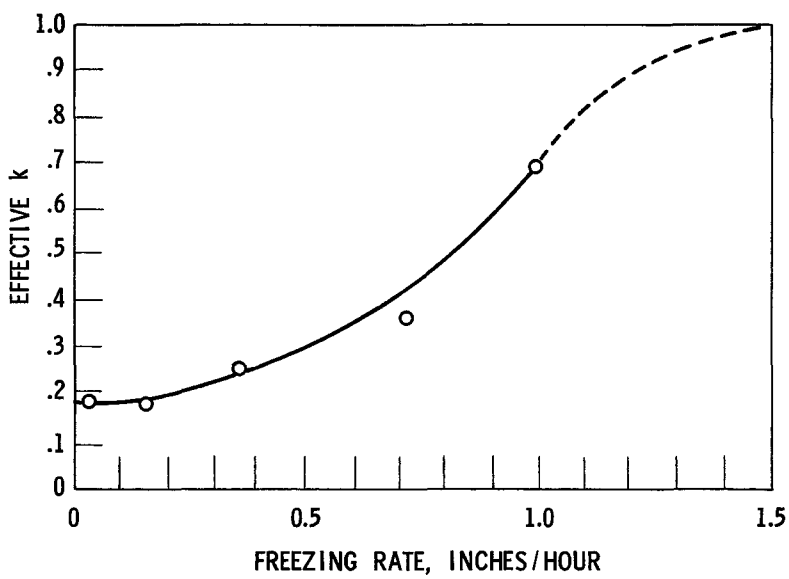

Figure 19

Effective Distribution Coefficient vs Rate of Solidification for K^+ in NaCl Solvent (After McFee, 3)

28

APPENDIX

Derivation of Equation 2

Let $k \equiv C_s/C_L$;
g = fraction of total volume solidified (Fig. 3);
C_s = gm/cc solute in solid at the liquid-solid interface;
C_L = gm/cc solute in the liquid after solidification has begun; (assumed uniformly distributed);
C_0 = gm/cc solute initially in the bar;
V_t = total volume of rod;
s = gm solute remaining in the liquid.

Assume (1) diffusion in the solid is negligible;
(2) complete mixing in the liquid;
(3) k is constant.

Then $C_s = k\, C_L$;

$$C_L = \frac{s}{(1-g)\, V_t} \quad ;$$

$$C_s = \frac{ks}{(1-g)\, V_t} \quad .$$

Let $V_t = 1$ cc. After a fraction, g, has frozen, freeze an additional amount, dg. C_s in dg is

$$C_s = -\frac{ds}{dg} \quad .$$

Now $ds = s_{(g)} - s_{(g+dg)}$,

where $s_{(g+dg)} > s_{(g)}$.

Therefore,

$$\frac{ks}{1-g} = -\frac{ds}{dg}$$

and

$$\int_{s_0}^{s} \frac{ds}{s} = \int_{0}^{g} \frac{-k\, dg}{(1-g)}$$

Then $\ln \frac{s}{s_0} = \ln (1-g)^k$

or $s = s_0 (1-g)^k$.

29

Substitution then gives

$$C_s = k\, s_0\, (1 - g)^{k-1} \quad .$$

Since $C_0 = \frac{s_0}{V_t}$

and $V_t = 1$ cc ,

$$C_s = k\, C_0\, (1 - g)^{k-1} \quad . \qquad \text{(Equation 2)}$$

Derivation of Equation 3, first pass

Let x = length solidified (Fig. 1);
z = length of molten zone;
L = total length of rod;
s = gm solute in zone, z, at any x ;
s_0 = gm solute in zone, z, at x = 0 ;
C_s = gm/cc solute in dx ;
C_L = gm/cc solute in zone z (assume uniform) ;
C_0 = gm/cc solute initially in rod ;
G = cross sectional area = 1 cm^2.

Assume $k < 1$; k, C_0, z, and G constant.
Diffusion in solid negligible and complete mixing in the liquid zone.
The last zone will be neglected in this derivation.

In Fig. 1 after an amount, x, has frozen, advance the zone a distance dx.
An amount, dx, will freeze and an equal volume, dz (= dx), will melt.
The amount of solute frozen (s_{dx}) is

$$s_{dx} = k\, C_L\, dx$$

where $C_L = \frac{s}{z}$.

The amount of solute melted (s_{dz}) at x + z is

$$s_{dz} = C_0\, dz = C_0\, dx,$$

since dz = dx.

The net change (ds) in s is

$$ds = (C_0 - \frac{ks}{z})\, dx \ ,$$

30

from which

$$\frac{ds}{dx} + \frac{k}{z} s = C_0$$

or

$$\frac{ds}{dx} + P(x)\, s = Q(x) \quad .$$

Let $s = uv$.

Then $\frac{ds}{dx} = u\frac{dv}{dx} + v\frac{du}{dx}$.

Substitution gives

$$v\frac{du}{dx} + u\frac{dv}{dx} + Puv = Q$$

or

$$v\frac{du}{dx} + \left(\frac{dv}{dx} + Pv\right) u = Q \quad .$$

Choose $v = e^{-\int P\, dx}$

so that

$$\frac{dv}{dx} + Pv = 0$$

$$\frac{dv}{v} = -\int P\, dx \quad .$$

Then

$$v\frac{du}{dx} = Q$$

$$du = \frac{Q}{v}\, dx$$

and $u = \int \frac{Q}{v}\, dx + D$.

Accordingly,

$$s = e^{-\int P\, dx}\left[\int Q\, e^{\int P dx}\, dx + D\right] \quad ,$$

$$s = De^{-\int_0^x P dx} + e^{-\int_0^x P dx}\left[\int_0^x Q\, e^{\int_0^x P dx}\, dx\right] \quad .$$

31

Since for the first pass, $P = \frac{k}{z} = \alpha$, and $Q = C_0$;

$$s_{(1)} = D_{(1)}\, e^{-\alpha x} + C_0 \frac{1}{\alpha}\,(1 - e^{-\alpha x})$$

where the subscript (1) refers to the first pass.

$$C_{s(1)} = \alpha s_{(1)} = C_0 + \left[D_{(1)}\alpha - C_0 \right] e^{-\alpha x}$$

$$\underline{C_{s(1)} = C_0 + \gamma\, e^{-\alpha x}} \qquad \text{(Equation 3)}$$

where

$$\gamma = D_{(1)}\,\alpha - C_0$$

$$D_{(1)} = z \int_0^{x=z} C_{s(0)}\, dx \quad .$$

Derivation of Equation 4, second pass.

The equation for $s_{(2)}$ may be developed as before and

$$s_{(2)} = D_{(2)}\, e^{-\int_0^x P dx} + e^{-\int_0^x P dx} \left[\int_0^x Q e^{\int_0^x P dx}\, dx \right]$$

where now

$$P = \frac{k}{z} = \alpha; \qquad Q = C_{s(1)} \text{ at } x + z \quad .$$

Thus

$$s_{(2)} = D_{(2)}\, e^{-\alpha x} + e^{-\alpha x} \left[\int_0^x \left[C_0 + \gamma\, e^{-\alpha (x+z)} \right] e^{\alpha x}\, dx \right]$$

or

$$s_{(2)} = \frac{1}{\alpha}\, C_0 + \frac{1}{\alpha}\,(\alpha\gamma\, x\, e^{-k} + \delta)\, e^{-\alpha x}$$

where

$$\delta = \left[D_{(2)}\alpha - C_0 \right]$$

and

$$D_{(2)} = z \int_0^{x=z} C_{s(1)}\, dx$$

$$C_{s(2)} = \alpha\, s_{(2)}$$

$$\underline{C_{s(2)} = C_0 + (\alpha\gamma\, x\, e^{-k} + \delta)\, e^{-\alpha x}} \qquad \text{(Equation 4)}$$

32

Derivation of Equation 5, third pass.

Here $P = \frac{k}{z} = \alpha$; $\quad Q = C_{s(2)}$ at $x + z$.

Now

$$s_{(3)} = D_{(3)}\, e^{-\alpha x} + e^{-\alpha x} \int_0^x C_{s(2)}\, e^{\alpha x}\, dx$$

$$s_{(3)} = D_{(3)}\, e^{-\alpha x} + e^{-\alpha x} \int_0^x \left\{ C_0 + \left[\alpha\, \gamma\, (x+z)\, e^{-k} + \delta\right] e^{-\alpha(x+z)} \right\} e^{\alpha x}\, dx$$

$$s_{(3)} = \frac{1}{\alpha}\, C_0 + \frac{1}{\alpha}\left[\alpha^2\, e^{-2k}\, \gamma \frac{(x+z)^2}{2} + \alpha\, e^{-k}\, \delta x + \epsilon\right] e^{-\alpha x}$$

where

$$\epsilon = D_{(3)}\, \alpha - C_0 - e^{-2k}\, \frac{k^2}{2}\, \gamma$$

$$D_{(3)} = z \int_0^{x=z} C_{s(2)}\, dx$$

$$\alpha s_{(3)} = C_{s(3)} = C_0 + \left(\alpha^2\, e^{-2k}\, \gamma \frac{(x+z)^2}{2} + \alpha\, e^{-k} \delta x + \epsilon\right) e^{-\alpha x} \quad \text{(Equation 5)}$$

Derivation of Equation 7, ultimate distribution.

The ultimate distribution after a certain minimum number of passes is defined as

$$C_s = F(x) \quad .$$

For a molten zone (of length z) to pass through this bar with no further change in concentration, the concentration of melting and freezing increments must be given by the equation above for ultimate distribution. The concentration in the liquid, C_L, is

$$C_L = \frac{1}{z} \int_x^{x+z} C_s\, dx = \frac{1}{z} \int_0^{x+z} F(x)\, dx \quad .$$

Since $C_s = k\, C_L$ by definition, we have

$$C_s = F(x) = \frac{k}{z} \int_x^{x+z} F(x)\, dx$$

33

a solution of which is

$$C_0 = Ae^{Bx} \qquad \text{(Equation 7)}$$

where

$$A = C_0 \frac{BL}{e^{BL}-1}$$

$$k = \frac{Bz}{e^{Bz}-1}$$

and

$$k < 1.$$

If $k > 1$, then

$$C_s = Ae^{-Bx} \qquad \text{(Equation 8)}$$

where

$$A = C_0 \frac{BL}{1 - e^{-BL}} = C_0\, BL$$

$$k = \frac{Bz}{1-e^{-Bz}} \approx Bz \quad .$$

Derivation of Equation 14, ratio of freezing rate to melting rate.

The equations presented in the text for the freezing rate and melting rate are

$$R_F = A_F\, G_F{}^{\nu} e^{-Q_F/RT} \qquad \text{(Equation 12)}$$

$$R_M = A_M\, G_M{}^{\nu}\, e^{-Q_M/RT} \quad . \qquad \text{(Equation 13)}$$

Using $Q_F \sim Q$ for diffusion in the liquid, and $Q_M - Q_F = L$ (latent heat of fusion), Chalmers[25] has calculated that

$$R_F = R_M = 3000 \text{ cm/sec}$$

for copper at the melting point.

The accommodation coefficients are related as follows:

$$\frac{A_M}{A_F} = e^{L/RT_e} \quad ,$$

where T_e is the equilibrium temperature of melting and freezing.

34

Then

$$\frac{R_F}{R_M} = \frac{A_F\, e^{-Q_F/RT}\,(G_F\nu)}{A_M\, e^{-Q_M/RT}\,(G_M\nu)}$$

$$= \frac{1}{e^{L/RT_e}} \cdot e^{-Q_F/RT + Q_M/RT}$$

$$= e^{(Q_M - Q_F/RT) - L/RT_e} \quad .$$

If $Q_M - Q_F = L$

$$\frac{R_F}{R_M} = \exp\left[\frac{L}{R}\left(\frac{1}{T} - \frac{1}{T_e}\right)\right] = e^{L(T_e - T)/R\,TT_e} \qquad \text{(Equation 14)}$$

If $T_e > T$, then $R_F > R_M$ and freezing will result.

If $T_e = 1406°K$, $T = 1405°K$, $L = 2.7$ k cal/mol, $R = 2$ cal/deg/mol,

$$\frac{R_F}{R_M} = e^{(1)(2700)/2(1405)(1406)} = e^{0.000683} = 1.0007 \quad .$$

Thus $R_F = 1.0007\, R_M$ for 1° of supercooling.

If $R_M = 3000$ cm/sec, then

$$R_F = 3002.1 \text{ cm/sec}$$

and $G = R_F - R_M = 3002.1 - 3000$

$$= 2.1 \text{ cm/sec.}$$

Calculation of G by Turnbull's Equation

$$G = \frac{\lambda kT}{h}\left(1 - e^{-\Delta F/RT}\right) \qquad \text{(Equation 15)}$$

$\lambda = 3.48\text{Å}$, $k = 1.39\ (10^{-16})$ erg/deg

$h = 6.6\ (10^{-27})$ erg sec, $T = 1406°K$

$R = 2$ cal/deg/mol, $\Delta H_f = 2.7$ kcal/mol

$$\Delta F \sim \frac{\Delta H_f \, \Delta T}{T_e} = \frac{2700(1)}{1406}$$

$$G = \frac{3.48\,(10^{-8})\;1.39\,(10^{-16})\;1406}{6.6\,(10^{-27})}\left[1 - e^{-\left(\frac{2700(1)}{1406} \cdot \frac{1}{2(1406)}\right)}\right]$$

$$= 1.03\,(10^{6})\left(1 - \frac{1}{1.0007}\right) = 1.03\,(10^{6})\,(0.0007)$$

$$= 721 \text{ cm/sec.}$$

BIBLIOGRAPHY

1. E. Scheuer, "Zum Kornseigerungsproblem," Ztsch.Metallkunde 23, 237 (1931).

2. J. Chipman and A. Hayes, "Mechanism of Solidification and Segregation in a Low Carbon Rimming Steel Ingot," Trans.A.I.M.E., 135, 85 (1939).

3. R. H. McFee, J. Chem. Phys., 15, 856 (1947).

4. W. G. Pfann, "Principles of Zone Melting," Trans.A.I.M.E., 194, 747 (1952).

5. W. G. Pfann, "Segregation of Two Solutes, with Particular Reference to Semiconductors," Trans.A.I.M.E., 194, 861 (1952).

6. W. G. Pfann and K. M. Olsen, "Purification and Prevention of Segregation in Single Crystals of Germanium," Phys. Rev., 89, 322 (1953).

7. W. G. Pfann, "Redistribution of Solutes by Formation and Solidification of a Molten Zone," Trans.A.I.M.E., 200, 294 (1954).

8. W. G. Pfann, A. J. Goss, and M. Tanenbaum, "Purification of Antimony and Tin by a New Method of Zone Refining," Trans.A.I.M.E., 200, 762 (1954).

9. W. G. Pfann, "Change in Ingot Shape During Zone Melting," J. of Met., 5, 1441 (1953).

10. E. E. Schumacher, "Ultra Pure Metals Produced by Zone Melting Technique," J. of Met. 5, 1428 (1953).

11. N. W. Lord, "Analysis of Molten Zone Refining," Trans.A.I.M.E., 197, 1531 (1953).

12. H. Reiss, "Mathematical Methods for Zone Melting Processes," Trans.A.I.M.E., 200, 1053 (1954).

13. B. Chalmers, W. A. Tiller, K. A. Jackson, and J. W. Rutter, "The Redistribution of Solute Atoms During Solidification of Metals," Acta Metallurgica, 1, 428 (1953).

14. B. Chalmers and J. W. Rutter, "A Prismatic Substructure Formed During Solidification of Metals," Can. J. Phys., 31, 15 (1953).

15. B. Chalmers and E. Teghtsoonian, "The Macro-mosaic Structure of Tin Single Crystals," Can. J. Phys., 29, 370 (1951).

37

16. B. Chalmers and F. Weinberg, "Dendritic Growth in Lead," Can. J. Phys., 29, 382 (1951).

17. B. Chalmers, M. T. Stewert, R. Thomas, K. Wauchope, and W. C. Winegard, "New Segregation Phenomena in Metals," Phys. Rev., 83, 657 (1951).

18. K. B. Pond and S. W. Kessler, "Model for Growth Form in Metals and Alloys." J. Met., 3, 1156 (1951).

19. B. H. Alexander and F. N. Rhines, "Dendritic Crystallization of Alloys," Trans. A.I.M.E., 188, 1267 (1950).

20. J. H. Holloman, "Heterogeneous Nucleation," Trans. A.S.M. 42A, 161 (1950).

21. D. Turnbull, "Principles of Solidification," Trans. A.S.M., 42A 282 (1950).

22. J. Frenkel, Kinetic Theory of Liquids, Oxford Univ. Press, London, 1946 p. 201.

23. W. Jost, Diffusion, Academy Press, New York, 1952, p. 479.

24. C. Wagner, "Theoretical Analysis of Diffusion of Solutes During The Solidification of Alloys," J. of Met., 6, 155 (1954).

25. B. Chalmers, "Melting and Freezing," J. of Met., 6, 519 (1954).

26. M. B. Bever and A. B. Michael, "Solidification of Al-rich Al-Cu Alloys," J. of Met. 6, 47 (1954).

27. C. A. Zapfee, "New Theory for the Solid State," Trans. A.S.M., 42, 387 (1950).

28. B. Chalmers and W. C. Winegard, "Supercooling and Dendritic Freezing in Alloys," Trans. A.S.M., 46, 1214 (1954).

29. B. Chalmers, Proc. Roy. Soc., 196, 64 (1949).

30. B. Chalmers and K. A. Jackson, "Influence of Striations on Plastic Deformation of Single Crystals of Tin," Can. J. Phys., 31, 1017 (1953).

31. B. Chalmers, "The Preparation of Single Crystals and Bi-Crystals by the Controlled Solidification of Metals," Can. J. Phys., 31, 132 (1953).

32. R. Hultgren and W. T. Olsen, "Effect of Rate of Freezing on Degree of Segregation in Alloys," Trans. A.I.M.E., 188, 1323 (1950).

38

33. E. Marburg, "Accelerated Solidification in Ingots; Its Influence on Ingot Soundness," Trans A.I.M.E., 191, 157 (1953).

34. W. S. Pellini, F. A. Brandt, and H. F. Bishop, "Solidification Mechanism of Steel Ingots," Trans A.I.M.E., 194, 44 (1952).

35. A. Prince, Discussion of Ref. 18, Trans A.I.M.E., 194, 1186 (1952).

36. A. J. Goss, Discussion of Ref. 18, Trans A.I.M.E., 194, 1187 (1952).

37. L. Burris, C. H. Stockman and I. G. Dillon, "Contribution to the Mathematics of Zone Melting," ANL-5294 (1954).

38. Desch, Chemistry of Solids, Cornell Press, Ithaca, New York 1934, p. 31.

39. C. S. Barrett, Structure of Metals, McGraw-Hill Book Co., New York, 1943, p. 436.

40. R. N. Hall, "Segregation of Impurities During the Growth of Germanium and Silicon Crystals," J. Phys. Chem., 57, 836 (1953).

41. J. A. Burton, R. C. Prin, and W. P. Slichter, "The Distribution of Solute in Crystals Grown From the Melt," J. Chem. Phys., 21, 1987 (1953).

42. R. E. Cech and D. Turnbull, "Microscopic Observation of the Solidification of Cu-Ni Alloy Droplets," Trans A.I.M.E., 189, 242 (1951).

43. R. W. Ruddle and A. Cibula, Discussion of Ref. 19, Trans A.I.M.E., 189, 561 (1951).